LETTER

Flexible Magnetic Microtubules Structured by Lipids and Magnetic Nanoparticles

Eun Chul Cho,*,† Jongwon Shim,‡ Kyeong Eun Lee,§ Jin-Woong Kim,‡ and Sung Sik Han§

Department of Biomedical Engineering, Washington University in St. Louis, 1 Brookings Drive, St. Louis, Missouri 63144, R&D Center, Amorepacific Corporation, 314-1 Bora-dong, Giheung-gu, Yongin 446-729, Korea, and School of Life Sciences and Biotechnology, Korea University, Anamdong, Seoul 136-701, Korea

ABSTRACT This study presents a microtubule that responds to a magnetic field. We made such a structure by incorporating iron oxide nanoparticles during the preparation of the microtubule. We found that the microtubule stretches its body when the magnetic field is applied and easily aligns with the direction of the applied magnetic field by rotating its body. When the magnetic field is removed, it loses its orientation and goes back to its original state by contraction. From the analysis of its magnetic response, we estimated that the magnetic microtubule had an elastic modulus of 33 MPa. Further analysis showed that the stretching and contracting of its body are due to its flexibility.

KEYWORDS: magnetic microtubules • lipids • iron oxide • flexibility

INTRODUCTION

In some cases, glycolipids, phospholipids, and fatty acids self-assemble into tubular forms when they are dispersed in aqueous media. The tubular forms usually result from the alignment of helical ribbons (1). The diameter and morphologies of these tubules are dependent on the molecular tilt, and this is influenced by the lipid characteristics, pH, salt, and temperatures (2−4). Lipid micro/nanotubules have been studied for a long time: they are comparable in structure with biological microtubules (consisting of tubulins) so they can be used as a biomimetic model (1, 5−8). Recently, they have also been used as a template for the fabrication of both inorganic nanostructures and protein/polymer assemblies (9−12). However, much attention has not been paid to the use of the mechanical properties of nanotubules. To date, there have been several attempts to measure the elastic modulus of natural microtubules, ranging from 7 GPa to 3 MPa (5, 13−15). A recent publication by Furusawa et al. showed that the elastic modulus of a synthetic lipid nanotubule is ~720 MPa, and they took advantage of such a moderate stiffness of the microtubule in the development of a microinjection method (16). Because the mechanical properties of most micro/nanotubules typically lie between the properties of glassy and rubbery polymers (17), we also thought that it would be possible to make a flexible hybrid microtubule that responds to an external stimulus.

In this letter, we present a microtubule that responds to a magnetic field. We made such a structure by incorporating iron oxide nanoparticles during the preparation of the microtubule. We found that the microtubule stretches its body when the magnetic field is applied and easily aligns with the direction of the applied magnetic field by rotating its body. When the magnetic field is removed, it loses its orientation and goes back to its original state by contraction. We carried out a further study on the physical and mechanical properties of the microtubule in order to discuss such a flexible change in the dimension of the microtubule in response to the magnetic field.

EXPERIMENTAL SECTION

Preparation of Magnetic Microtubules. We prepared magnetic microtubules by modifying a method reported in ref 18. Briefly, magnetic microtubules were prepared by heating 5 g of 12-hydroxystearic acid (HSA; 70% purity; Wako Chemicals, Osaka, Japan) above 80 °C in 95 mL of an aqueous 1 M ethanolamine (EA) solution for 30 min and then adding 5 mL of 2 wt % iron(III) oxide nanoparticles [Aldrich, 14.1 ± 3.2 nm by transmission electron microscopy (TEM) analysis] in an aqueous dispersion. After mixing for 15−20 min, the dispersion was cooled to room temperature. Microtubules without iron oxide nanoparticles were prepared with the same procedure, except that the iron oxide nanoparticle dispersion was not added.

Characterization of Microtubules. The morphologies of the microtubules were observed by both optical microscopy and cryo-TEM. For a cryo-TEM experiment, a drop of fluid (about 7 μL) was placed on a grid with holes. The grid was then immediately plunged into liquid ethane. The frozen grids were stored in liquid nitrogen and transferred in a Gatan model 630 cryotransfer (Gatan, Inc., Warrendale, PA) under liquid nitrogen at approximately −185 °C. Samples were observed at approximately −170 °C using a Tecnai 12 electron microscope (Philips, Eindhoven, The Netherlands) at 120 kV, and the images were acquired with a Multiscan 600W CCD camera (Gatan, Inc., Warrendale, PA). Energy-dispersive X-ray spectroscopy (EDX; AMETEK Materials Analysis Division, Mahwah, NJ) was used for the elemental analysis of the magnetic microtubules. The orientation of the magnetic microtubules in response to a magnet was observed by an optical microscope (Olympus BX-100). For this experiment, we moved a magnet around a microscope slide that contained magnetic microtubules (see Figure 2A) and observed the alignment of the magnetic microtubules at each direction of the magnet. We also used the optical microscope for viewing the morphological changes of the microtubules [made with EA and potassium hydroxide (KOH)] after sonicating them for 60 min. Differential

* Corresponding author. E-mail: choe@seas.wustl.edu.
Received for review March 3, 2009 and accepted May 5, 2009
† Washington University of St. Louis.
‡ Amorepacific Corp.
§ Korea University.
DOI: 10.1021/am900139b

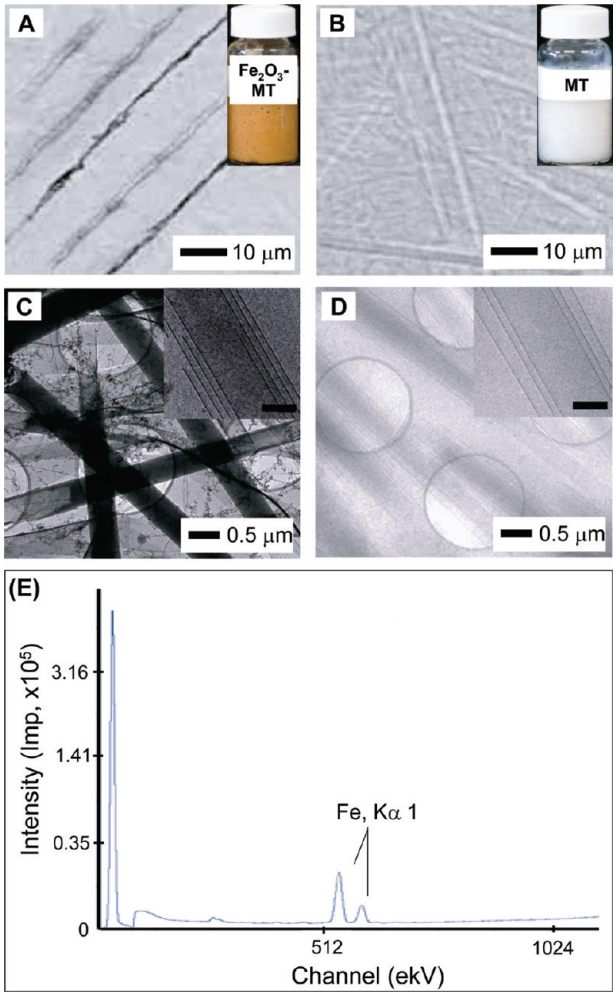

FIGURE 1. (A and B) Optical micrographs for HSA microtubules with (A) and without (B) iron oxide. Insets: photographs of each microtubule. (C and D) Cryo-TEM micrographs for the HSA microtubule with (C) and without (D) iron oxide nanoparticles. Inset (scale bar: 0.2 μm): high magnification images of each microtubule. (E) Analysis of EDX on the HSA microtubules with iron oxide.

scanning calorimetry (DSC Q1000) was used for studying the thermal behavior of the two microtubules. We scanned from 20 to 100 °C with a scanning rate of 1 °C/min. To prevent the evaporation of water, we used high-volume pans.

RESULTS AND DISCUSSION

We prepared magnetic microtubules in an aqueous EA solution by heating a fatty acid (HSA), adding iron oxide nanoparticles, and subsequently cooling the mixture to room temperature. The synthesis of lipid microtubules based on HSA and EA was described by Douliez et al. (18), and we modified the method to prepare the magnetic microtubules. Because the melting temperature of HSA is ~77 °C (by DSC), heating HSA above its melting temperature (80–85 °C) enabled HSA to be homogeneously dispersed by stirring of the mixture. We found that the solubility of HSA in water at these temperatures highly depended on the type of base. We tested with three bases [KOH, EA, and triethanolamine (TEA)], and we obtained the clearest solution with KOH. We observed a bluish solution when using EA, indicating that HSA molecules were assembled to form micelles or vesicles. Use of TEA resulted in a turbid solution because of the formation of large aggregates of HSA.

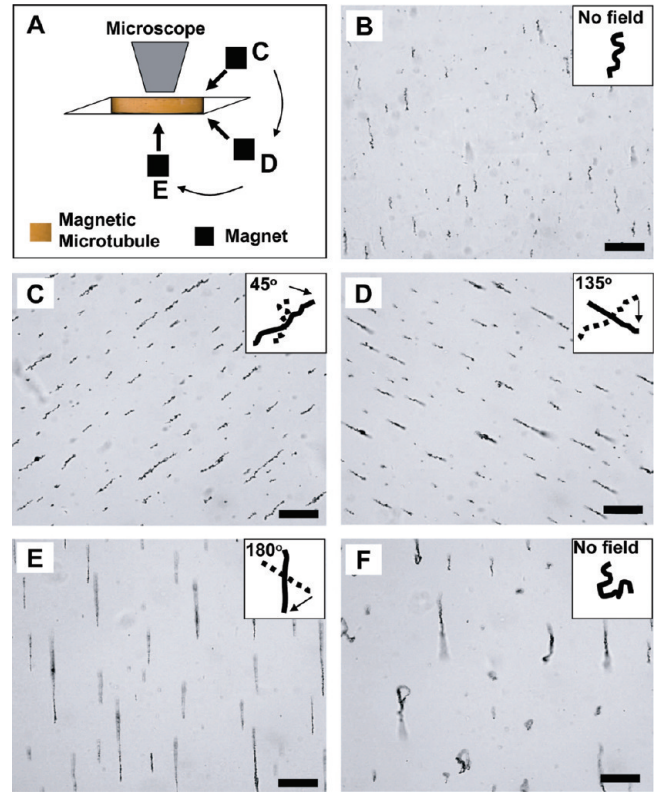

FIGURE 2. (A) Experimental setup for observation of the magnetic microtubules oriented to a magnetic field. (B–F) Response of magnetic microtubules toward the magnetic field: (B) no field, (C) 45° direction, (D) 135° direction, (E) 180° direction. After removal of the field (F), the magnetic microtubules are disoriented and contracted. The scale bar is 20 μm. Arrows indicate the directions to which the magnet or microtubules rotate.

The different solvation power of these bases for HSA resulted in different microstructures when the aqueous dispersions were cooled to room temperature (see Figure S1 in the the Supporting Information). We chose EA as a base because it yielded reproducible microtubules, which were transformed from micelles or vesicles during the cooling process (19). Different concentrations also influenced the morphology of the microtubules. In this study, the concentration of HSA was 5 wt %. While heating HSA above its melting temperature, the iron(III) oxide nanoparticles were added to the aqueous HSA dispersion. Cooling the mixture to room temperature resulted in a brownish, viscous fluid (inset in Figure 1A).

Parts A and B of Figure 1 show the optical micrographs of the microtubules with or without iron oxide nanoparticles. They had the same tubular structures, but the wall of the microtubules with iron oxide nanoparticles looked darker than that without nanoparticles. This difference indicated that the iron oxide nanoparticles were adsorbed on the walls of the microtubules. We further investigated the structures of these microtubules by cryo-TEM, as shown in Figure 1C,D. The two microtubules had in common an outer diameter of ~0.5 μm and multiwalled structures (3–4 walls). Jean et al. reported that these multiwalled tubules were made of a planar sheet rolled onto them and resulted from a metastable state of single-walled nanotubules (20). We did not observe any evidence of membrane twists, as reported in other literature (1, 4, 18a, 19, 21), probably because of the

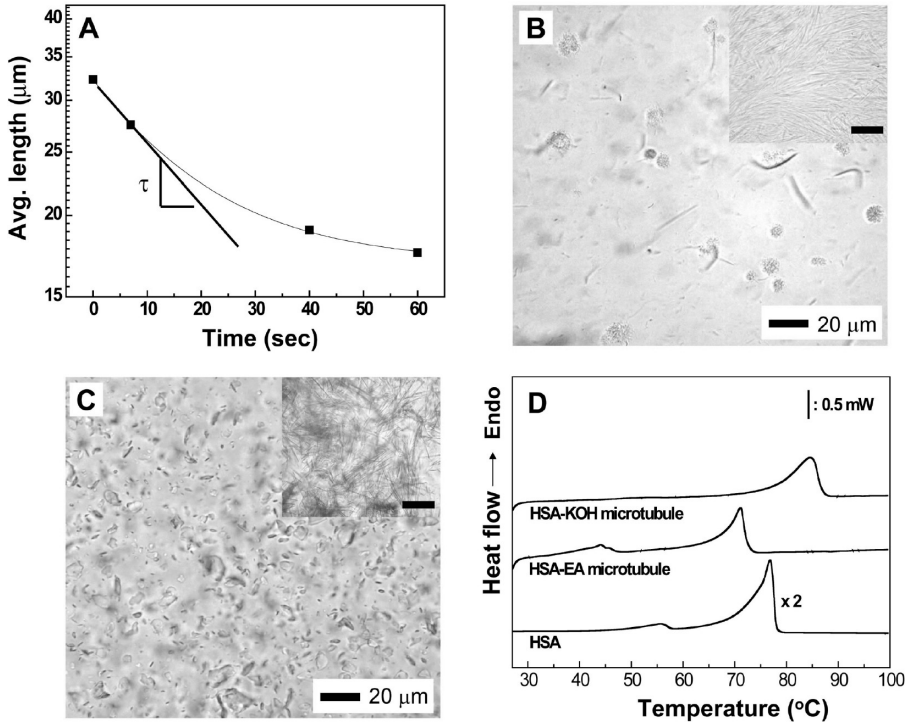

FIGURE 3. (A) Plot showing time-dependent changes in the average length of the magnetic microtubules when a magnet was removed from the direction of 180°. Insets: representative micrographs at each time. (B and C) Optical micrographs for the microtubules (without iron oxide) after sonication for 60 min: (B) microtubules made with EA and (C) those made with KOH. Insets: micrographs before sonication (also see the Supporting Information). The scale bar is 20 μm. (D) DSC thermograms for HSA, HSA microtubules made with EA, and those made with KOH. The scanning rate was 1 °C/min, and the samples were scanned from 25 to 100 °C.

widening of helical ribbons with constant helical pitch (1). On the basis of the analysis of Figure 1C,D, we also found that the microtubules with iron oxide looked darker than those without iron oxide. We could not clearly distinguish the iron oxide nanoparticles adsorbed from the microtubules with cryo-TEM. However, further analysis of EDX in Figure 1C showed that the dark color was due to the existence of iron oxide (Figure 1E). However, some nanoparticles were aggregated outside the microtubules, indicating that not all of the iron oxide nanoparticles were adsorbed on the walls of the microtubules.

We next investigated the responsiveness of the magnetic microtubules to a magnetic field by using a magnet, as shown schematically in Figure 2A. The magnetic microtubule fluid was dropped onto a glass slide, and the magnet was moved around the fluid. When there was no magnetic field, the microtubules showed no specific orientation (Figure 2B). In contrast, when the magnet was brought close, the magnetic microtubules were oriented toward the magnet (Figure 2C−E). We applied the magnet first in the 45° direction (Figure 2C) and then turned its position clockwise to 135°, followed by 180°. In following the magnet, the magnetic microtubules turned their bodies to point one end toward the magnet. Interestingly, it was observed that the magnetic microtubules stretched their bodies in 1−2 min while the magnetic fields were applied (Figure 2D,E). When the magnet was removed from the vicinity of the microtubule fluid (Figure 2F), the microtubules lost their orientations and their stretched bodies became shortened within 1 min: most of the microtubules looked either slightly or completely contracted, although a few tubules were still in the stretched condition. This result demonstrates that the microtubules can freely stretch and contract their bodies. For comparison, we observed the movement of free, nonadsorbed iron oxide nanoparticles under the magnetic field, and the aggregates of nanoparticles just moved toward the magnet (see Figure S2 in the Supporting Information).

It is thought that the coil-like microtubules with magnetic nanoparticles attached to them become straight upon application of the magnetic field because the nanoparticles are attracted to the field. In addition, they go back to the original condition by curling of the microtubules after removal of the magnetic field. We believe that switching from the original state to the stretched state (or vice versa) of the microtubules is only possible when the microtubules are flexible. On this thought, we tried to estimate the elastic modulus of the magnetic microtubules by measuring the average length of the microtubules from 0 s (Figure 2E) to 60 s (Figure 2F) after removal of the magnetic field. The average lengths are plotted in Figure 3A. We obtained the relaxation time (τ) for contraction of the microtubules as 19.4 s, and the elastic modulus of the microtubules was determined by using equations in ref 16 as 33.0 MPa (see the Supporting Information). Note that this value is for the microtubules reinforced by iron oxide nanoparticles, so that the modulus of pure lipid microtubules is probably lower than this value, based on the equation suggested by Nielsen (22). However, we expect that the effect of iron oxide nanoparticles on the elastic modulus of the magnetic microtubules is not significant because the concentration (or volume fraction) of the iron oxide in the

magnetic microtubules would be a maximum of 2 wt %. We compared the modulus with those in other references. This one is 1 order of magnitude lower than the value for the microtubules of glycolipids by Furusawa et al. (16) and is in the range of natural microtubules (13, 15). This value is also close to that of synthetic rubber, polyurethane (23), so we expect that these microtubules will have mechanical properties between those of ductile semicrystalline polymers (0.1−1 GPa) and rubbers (0.1−1 MPa) (17). Therefore, we suggest that stretching and recoiling of the magnetic microtubules are possible because these microtubules are flexible.

We confirmed the flexibility of the magnetic microtubules by observing the morphologies of microtubules (without iron oxide) after sonication (Figure 3B; also see Figure S3 in the Supporting Information). The inset in Figure 2B is the microtubules before sonication. After sonication of the microtubules for 60 min, it can be seen that the tubular structures are bent or transformed to spherical vesicles. This transformation was also found in the work by Nakashima et al., in which they warmed the helical nanotubules above the phase transition temperatures (4). For comparison, we also sonicated microtubules made with KOH (Figure 3C). After sonication, in contrast to microtubules with EA, most microtubules were broken. It is thought that the different results for the two microtubules are caused by different mechanical properties: after energy is applied, the flexible microtubules made with EA dissipate the energy by deforming their bodies but the microtubules made with KOH are brittle enough for their bodies to be fractured by external energy (17, 24). Because the mechanical properties of the materials are closely related to their microstructures (i.e., chain configuration, crystalline structure, and melting temperature) (25−27), we further investigated the thermal behavior of the two microtubules to see if they show any differences in structure (Figure 3D). It can be clearly seen that the two microtubules have different melting temperatures: the microtubules with EA have two melting peaks at 43 °C (20% melted) and 71 °C (80% melted). In contrast, the microtubules with KOH show only one melting temperature of 85 °C. Douliez et al. reported a similar result in the HSA microtubules with EA, and they suggested that the peak at 43 °C was due to a gel-to-fluid lipid phase transition and the peak at 71 °C was due to lipid melting (18b). The results suggest that the two microtubules have different phase behaviors and crystalline structures. Specifically, the microtubules made with EA would be partially fluidlike, while the microtubules with KOH are in a gel-like state at room temperature. From the above results, one can say that it is likely that the different mechanical properties of the two microtubules are attributed to the different microstructures of the microtubules.

In summary, we demonstrated that microtubules with adsorbed iron oxide nanoparticles can respond to the magnetic field, and they move freely toward the magnetic field by stretching and going back to their original bodies flexibly. We are currently focusing on preparing many more uniform-sized magnetic microtubules to be potentially used as magnetically responsive tips and tweezers and in other applications in biomedical fields.

Supporting Information Available: Optical microscopic images for microtubules with different bases and for the response of magnetic nanoparticles to a magnet and equations for the elastic modulus of magnetic microtubules. This material is available free of charge via the Internet at http://pubs.acs.org.

REFERENCES AND NOTES

(1) Shimizu, T.; Masuda, M.; Minamikawa, H. *Chem. Rev.* **2005**, *105*, 1401.
(2) Israellachvili, J. *Intermolecular and Surface Forces*; Academic Press: San Diego, 1998.
(3) (a) Yager, P.; Schoen, P. E. *Mol. Cryst. Liq. Cryst.* **1984**, *106*, 371. (b) Yager, P.; Schoen, P. E.; Davies, C.; Price, R.; Singh, A. *Biophys. J.* **1985**, *48*, 899. (c) Schoen, P. E.; Yager, P. *J. Polym. Sci., Polym. Phys. Ed.* **1985**, *23*, 2203. (d) Yamada, K.; Ihara, H.; Ide, T.; Fukumoto, T.; Hirayama, C. *Chem. Lett.* **1984**, 1713. (e) Nakashima, N.; Asakuma, S.; Kim, J.-M.; Kunitake, T. *Chem. Lett.* **1984**, 1709.
(4) Nakashima, N.; Asakuma, S.; Kunitake, T. *J. Am. Chem. Soc.* **1985**, *107*, 509.
(5) Gittes, F.; Mickey, B.; Nettleton, J.; Howard, J. *J. Cell Biol.* **1993**, *120*, 923.
(6) Yeager, M.; Wilson-Kubalek, E. M.; Weiner, S. G.; Brown, P. O.; Rein, A. *Proc. Natl. Acad. Sci. U.S.A.* **1998**, *95*, 7299.
(7) Lopez, C. F.; Nielsen, S. O.; Moore, P. B.; Klein, M. L. *Proc. Natl. Acad. Sci. U.S.A.* **2004**, *101*, 4431.
(8) (a) Curatolo, W. *Biochim. Biophys. Acta* **1987**, *906*, 111. (b) Curatolo, W. *Biochim. Biophys. Acta* **1987**, *906*, 137.
(9) Schnur, J. M.; Price, R.; Schoen, P.; Yager, P.; Calvert, J. M.; Georger, J.; Singh, A. *Thin Solid Films* **1987**, *152*, 181.
(10) (a) Archibald, D. D.; Mann, S. *Nature* **1993**, *364*, 430. (b) Burkett, S. L.; Mann, S. *Chem. Commun.* **1996**, *3*, 321.
(11) (a) Boal, A. K.; Headley, T. J.; Tissot, R. G.; Bunker, B. C. *Adv. Funct. Mater.* **2004**, *14*, 19. (b) Wang, Z.; Ho, K. J.; Medforth, C. J.; Shelnutt, J. A. *Adv. Mater.* **2006**, *18*, 2557.
(12) Wilson-Kubalek, E. M.; Brown, R. E.; Celia, H.; Milligan, R. A. *Proc. Natl. Acad. Sci. U.S.A.* **1998**, *95*, 8040.
(13) Vinckier, A.; Dumortier, C.; Engelborghs, Y.; Hellenmans, L. *J. Vac. Sci. Technol. B* **1996**, *14*, 1427.
(14) Kurachi, M.; Hiroshi, M.; Tashiro, M. *Cell Motil. Cytoskeleton* **1995**, *30*, 221.
(15) Kis, A.; Kasas, S.; Kulik, A. J.; Catsicas, S.; Forro, L. *Langmuir* **2008**, *24*, 6176.
(16) Furusawa, H.; Fukagawa, A.; Ikeda, Y.; Araki, J.; Ito, K.; John, G.; Shimizu, T. *Angew. Chem., Int. Ed.* **2003**, *42*, 72.
(17) Young, R. J.; Lovell, P. A. *Introduction to Polymers*, 2nd ed.; CRC Press: London, 1991.
(18) (a) Douliez, J.-P.; Gaillard, C.; Nvailles, L.; Nallet, F. *Langmuir* **2006**, *22*, 2942. (b) Douliez, J.-P.; Pontoire, B.; Gaillard, C. *ChemPhysChem* **2006**, *7*, 2071.
(19) Dung, D. S.; Benedek, G. B.; Konikoff, F. M.; Donovan, J. M. *Proc. Natl. Acad. Sci. U.S.A.* **1993**, *90*, 11341.
(20) Jean, B.; Oss-Ronen, L.; Terech, P.; Talmon, Y. *Adv. Mater.* **2005**, *17*, 728.
(21) Selinger, J. V.; Schnur, J. M. *Phys. Rev. Lett.* **1993**, *71*, 4091.
(22) Nielsen, L. E. *J. Appl. Phys.* **1970**, *41*, 4626.
(23) Xu, M.; Zhang, T.; Gu, B.; Wu, J.; Chen, Q. *Macromolecules* **2006**, *39*, 3540.
(24) Chen, H.; Wu, J. *Macromolecules* **2007**, *40*, 4322.
(25) (a) Cerrada, P.; Oriol, L.; Piñol, M.; Serrano, J. L.; Iribarren, I.; Muñoz Guerra, S. *Macromolecules* **1996**, *29*, 2515. (b) Arnold, J. C. *Polym. Eng. Sci.* **1995**, *35*, 165. (c) Pluta, M.; Galeski, A. *Biomacromolecules* **2007**, *8*, 1836.
(26) (a) Chen, Y. L.; Helm, C. A.; Israelachvili, J. N. *J. Phys. Chem.* **1991**, *95*, 10736. (b) Lee, D. H.; Kim, D.; Oh, T.; Cho, K. *Langmuir* **2004**, *20*, 8124.
(27) (a) Bernsdorff, C.; Winter, R. *J. Phys. Chem. B* **2003**, *107*, 10658. (b) Cho, E. C.; Lim, H. J.; Shim, J.; Park, J. Y.; Dan, N.; Kim, J.; Chang, I.-S. *J. Colloid Interface Sci.* **2007**, *311*, 243.

AM900139B